Interdisciplinary Information Sciences Vol. 15, No. 2 (2009) 301–318

ISSN 1340-9050 print/1347-6157 online
DOI 10.4036/iis.2009.301

Solvable Probabilistic Model for Cycles in Planar Graph

Kazuyuki TANAKA[1*] and Valery VAN KERREBROECK[2]

[1]*Department of Applied Information Sciences, Graduate School of Information Sciences, Tohoku University, 6-3-09 Aramaki-aza-aoba, Aoba-ku, Sendai 980-8579, Japan*
[2]*Dipartimento di Fisica, SMC-INFM-CNR and INFN, Sapienza Università di Roma, P. A. Moro 2, 00185 Roma, Italy*

Received January 19, 2009; final version accepted February 26, 2009

We study a probabilistic model for single connected cycles on an undirected planar graph for which the degree of every vertex is restricted to two or three. By using a diagrammatical method to solve a free fermion model, we derive the exact expression of the partition function as well as marginal probabilities. We compare the exact results for the marginals with the approximations obtained with Loopy Belief Propagation allowing us to evaluate the efficacy of the latter.

KEYWORDS: probabilistic information processing, statistical inference, Bayesian network, free fermion model, loopy belief propagation, statistical mechanics, advanced mean-field method

1. Introduction

Recently, probabilistic analysis of constraint satisfaction problems has been performed using concepts of spin glass theory and phase transitions [1–3]. Solving these problems exactly requires an exponential order of computational time. Marinari, Semerjian and Van Kerrebroeck have studied the problem of finding long cycles in random graphs by treating them as a constraint satisfaction problems [4, 5]. They introduced a probabilistic model identifying the long cycles and employed loopy belief propagation (LBP) and Markov chain Monte Carlo to analyze associated problems.

One of the solvable probabilistic models is a vertex model with a free fermion condition on the undirected planar graph [6, 7]. It is referred to as a *free fermion model*. Such a vertex model has been investigated also on the honeycomb lattice and the exact expression of the free energy in the thermodynamic limit has been derived [8, 9]. The partition function of the free fermion model on a square lattice can be expressed in terms of a summation of cycles on the undirected planar graph and can be calculated analytically by using a diagrammatical method [10, 11]. The justification of the diagrammatical method for free fermion models on any planar graph has been given in Refs. [12–14]. The same results for the partition function of the free fermion model on any planar graphs can be derived by using Grassmann variables [15, 16]. It has been suggested that the partition function can be reduced also to some well-known integrable representations of quantum field theory in terms of Hamiltonian matrices [18–20]. These methods have allowed to calculate the partition function exactly both from the point of view of computational theory and statistical learning theory [17, 21, 22].

By using the diagrammatical method [12–14], the partition functions of the free fermion models, including some two-dimensional Ising models on planar graphs, are expressed in terms of contributions of all the simple cycles. The practical algorithms to calculate the exact value of the free energy can be reduced to the computations of the determinants of the matrices of random walks. The justification for the diagrammatical method has been done only for planar graphs. Using the diagrammatical method, the probabilistic models can be reduced to the free fermion models if they satisfy also some additional conditions which are valid for all the states at each vertex. Some of the additional conditions are referred to as free fermion conditions. Free fermion conditions have to be imposed on all the states at every vertex if they have a degree of at least four. However, all the states at every vertex with degree two or three do not have to satisfy such additional conditions to derive the exact expression of the free energy. By restricting the graphs to the planar graphs with the degree being two or three, the probabilistic model formulated to find long cycles in graphs in Ref. [4] can be solved exactly by means of the diagrammatical method. It is interesting to derive the exact expressions of the partition functions for solvable probabilistic models to find long cycles in graphs and compare the exact results with the approximate ones obtained by using LBP.

In the present paper, we introduce an undirected planar graph for which the degree of every vertex is restricted to two or three. On the undirected planar graph, we consider a probabilistic model for single connected cycles. By using a diagrammatical method to solve free fermion models, we derive the exact expression of the partition function as well as

* Corresponding author. E-mail: kazu@smapip.is.tohoku.ac.jp, Webpage: http://www.smapip.is.tohoku.ac.jp/~kazu/

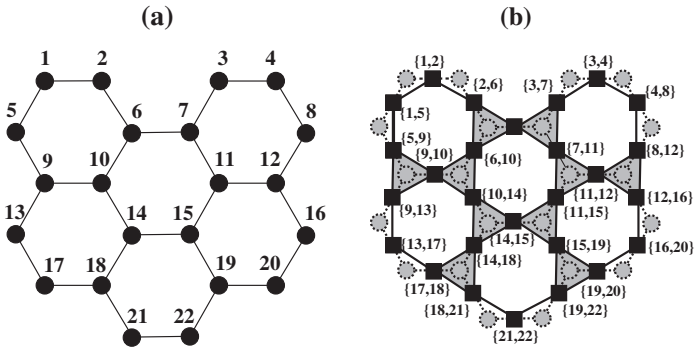

Fig. 1. Graph consisting of vertices with degree 2 or 3 and the present probabilistic model on the graph. (a) Graph consisting of vertices with degree 2 or 3. Solid circles and thin line segments denote vertices and edges, respectively. (b) Probabilistic model for cycles of the graph given in (a). Random variables $S_{ij}(= 0, 1)$ are assigned to all edges. Each triangular denotes an interaction among the three edges it includes. Each thick line segment denotes an interaction between the two edges it connects.

marginal probabilities. In Sec. 2, we define the probabilistic model on the undirected planar graph. In Sec. 3, we rewrite the partition function of the probabilistic model by the diagrammatical representation and reduce it to a determinant by using the diagrammatical method given in [10–13]. By using the expression of the partition function, we derive the marginal probability that a fixed edge is included by one of the cycles. In Sec. 4, the exact expression for the marginal probabilities are derived by using the diagrammatical method and the discrete Fourier transformation on an infinite honeycomb lattice. In Sec. 5, we derive the approximate value of the marginal probability that a fixed edge is included by one of the cycles by using the LBP on an infinite honeycomb lattice. In Sec. 6, we give some numerical results for finite planar graphs. In Sec. 7, we analyze the asymptotic behaviour of the marginal probabilities near a special value of an external parameter for finite planar graphs. In Sec. 8, we give some concluding remarks.

2. Cycle Graph on Undirected Planar Graph

In this section, we define a probabilistic model for identifying cycles on an undirected planar graph. In order to obtain exact results by means of the diagrammatical method given in [11–14], we restrict the degree of every vertex to two or three.

We consider an undirected planar graph $G = (V, E)$ consisting of N vertices without closed one-edge loops and multiple edges. Here $V \equiv \{i \mid i = 1, 2, \cdots, N\}$ is a set of all vertices and $E \subset \{\{i, j\} \mid 1 \leq i < j \leq N\}$ is a set of edges. Note that no pair of edges can intersect with each other on a planar graph. A set of neighbouring vertices of the vertex i is denoted by ∂i. In this paper, we restrict $|\partial i| = 2, 3$ and denote the set of vertices i for which the degree $|\partial i|$ is two in the graph $G = (V, E)$ by $\partial V \equiv \{i \mid |\partial i| = 2\}$.

In the free fermion model, we distinguish two kinds of states of each edge. One is represented by a solid line segment and is referred to as a *solid edge*. Another one is represented by a dashed line segment and is referred to as a *dashed edge*. We consider the configuration of a vertex to be determined by the solid edges connected to the vertex, and the configuration of the system is determined by the set of vertex configurations for all the vertices. We only allow for such vertex configurations for which there exist none or an even number of solid edges connected to every neighbouring vertex. The random variable associated to each edge $\{i, j\} \in E$ is denoted by S_{ij}, which takes 1 for the solid edge and 0 for the dashed edge, respectively. The set of all the random variables $\{S_{ij} \mid \{i, j\} \in E\}$ is denoted by the vector $\boldsymbol{S}$. The state variable of edge $\{i, j\} \in E$ is denoted by s_{ij}. All the possible states of the vertices of the graph given in Fig. 1 are shown in Figs. 2 and 3. Some possible configurations are shown in Fig. 4.

The probability distribution for every configuration $\boldsymbol{s} \equiv \{s_{ij} \mid \{i, j\} \in E\}$ is expressed as follows, as a function of an external parameter u,

$$\Pr\{\boldsymbol{S} = \boldsymbol{s} \mid u\} \equiv \frac{1}{Z(u)} \left(\prod_{\{i,j\} \in E} u^{s_{ij}} \right) \left(\prod_{i \in V} \left(\delta\left(\sum_{k \in \partial i} s_{ik}, 0 \right) + \delta\left(\sum_{k \in \partial i} s_{ik}, 2 \right) \right) \right) \tag{1}$$

where $\delta(a, b) = \delta_{a,b}$ is the Kronecker delta and $Z(u)$ is the partition function defined by

$$Z(u) \equiv \sum_{\boldsymbol{s}} \left(\prod_{\{i,j\} \in E} u^{s_{ij}} \right) \left(\prod_{i \in V} \left(\delta\left(\sum_{k \in \partial i} s_{ik}, 0 \right) + \delta\left(\sum_{k \in \partial i} s_{ik}, 2 \right) \right) \right) \tag{2}$$

The summation $\sum_{\boldsymbol{s}} \equiv \sum_{\{s_{kl}=0,1 \mid \{k,l\} \in E\}}$ is taken with respect to all the edge variables for edges in the set E. In the limit of $u \to +\infty$, only configurations in which all vertices have two solid edges appear in this probabilistic model. In the case of $u \to 0$, only the configuration with no solid edges appears.

One quantity we focus on in particular is the marginal expressing the probability with which an edge is included by any of the cycles,

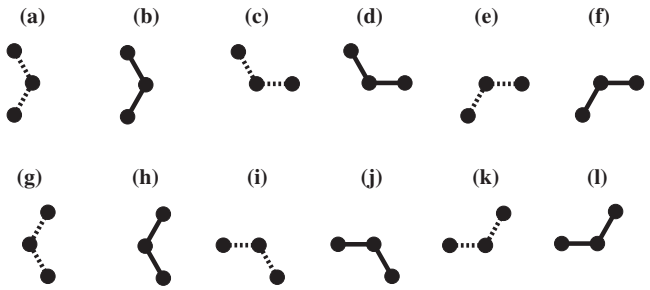

Fig. 2. All possible states of vertices with degree 2 on the graph given in Fig. 1.

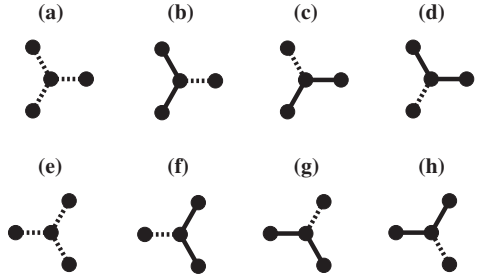

Fig. 3. All possible states of vertices with degree 3 on the graph given in Fig. 1.

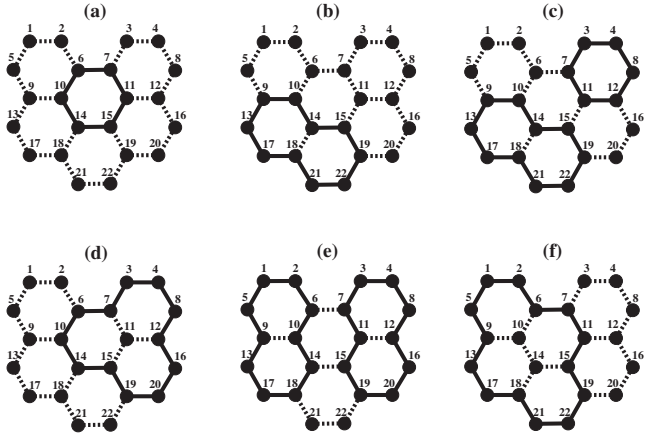

Fig. 4. Examples of the possible configurations on the graph given in Fig. 1. The numerators $(\prod_{\{i,j\}\in E} u^{s_{ij}})(\prod_{i\in V}(\delta(\sum_{k\in\partial i} s_{ik}, 0) + \delta(\sum_{k\in\partial i} s_{ik}, 2)))$ in Eq. (1) for the configurations (a)–(f) are (a) u^6, (b) u^{10}, (c) u^{16}, (d) u^{12}, (e) u^{20} and (f) u^{14}, respectively.

$$\Pr\{S_{ij} = 1 \mid u\} \equiv \sum_{\boldsymbol{s}} \delta(s_{ij}, 1) \Pr\{\boldsymbol{S} = \boldsymbol{s} \mid u\} = \sum_{\boldsymbol{s}} s_{ij} \Pr\{\boldsymbol{S} = \boldsymbol{s} \mid u\}. \tag{3}$$

By differentiating $\ln(Z(u))$ with respect to u, we obtain

$$\sum_{\{i,j\}\in E} \Pr\{S_{ij} = 1 \mid u\} = u \frac{\partial}{\partial u} \ln Z(u). \tag{4}$$

The latter equality is derived by differentiating both sides of Eq. (2) with respect to u and by using Eq. (3).

3. Partition Function for Free Fermion Model on Planar Graph

In this section, we give the exact expression of partition functions for the probabilistic model defined in the previous section. The explicit expression can be derived in a similar way as the scheme presented in [12, 13]. We briefly summarize the derivation in the present section.

The partition function $Z(u)$ can be represented as

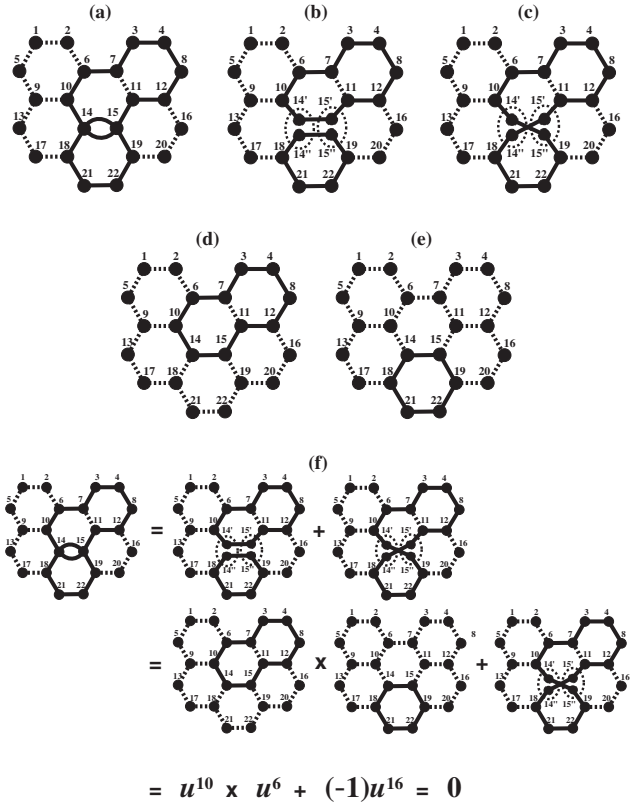

Fig. 5. An example of configurations including one double solid edge and their replacements. A double solid edge $\{14, 15\}$ in (a) can be replaced by two kinds of sets, $\{\{14', 15'\}, \{14'', 15''\}\}$ and $\{\{14', 15''\}, \{14'', 15'\}\}$ as shown in (b) and (c). The contribution for configuration (a) is replaced by the sum of contributions (b) and (c). We see that there occurs one crossing in (c). The configuration in (c) consists of two cycles of solid edges in (d) and (e) and the contribution is the product of the contributions of (d) and (e). The contribution for configuration (a) is derived as shown in (f) and is equal to zero because a cycle of solid edges includes an additional factor $(-1)^r$ if there are r crossings in the cycle.

$$Z(u) = 1 + \{\text{the sum of all those single connected configurations on the undirected planar graph, such that every vertex is connected to none or two solid edges}\}. \tag{5}$$

A configuration in Eq. (5) denotes the product of the factors u for edges $\{i, j\}$ in it. The single connected configurations are those including only cycles of solid edges which are pairwise connected at the vertices, without allowing for multiple solid edges. Multiple solid edges are the states in which a pair of neighbouring vertices are connected by two or more solid edges. Some examples of configurations including multiple solid edges are shown in Figs. 5(a) and 6(a). The multiple solid edges appear in $\{14, 15\}$ of Fig. 5(a), and in $\{10, 14\}$ and $\{14, 15\}$ of Fig. 6(a), respectively. These configurations are forbidden in the set of all the single connected configurations in Eq. (5).

Eq. (5) can be regarded as

$$Z(u) = 1 + \{\text{the sum of all the products of cycles of solid edges which are pairwise connected at the vertices, without allowing for multiple solid edges}\}. \tag{6}$$

We remark that all the possible configurations do not include any vertex state which have more than two solid edge states in the present graph. If we walk in one direction along any of the cycles of solid edges of all the possible configurations until we return to the initial vertex, no other vertices but the initial and terminal vertex will be encountered twice or more. Such cycles of solid edges are referred to as simple cycles. Thus the possible configurations consist only of simple cycles.

Now we consider all the cycles that allow for multiple solid edges. Each vertex i connected to a double solid edge is divided into two vertices i' and i''. A double solid edge $\{i, j\}$ can be replaced by two kinds of sets, $\{\{i', j'\}, \{i'', j''\}\}$ and $\{\{i', j''\}, \{i'', j'\}\}$. In this replacement, there may occur crossings in a cycle of solid edges. A cycle of solid edges is characterized by the product of the following factors:

(1) $+1$ and -1 depending on whether the parity of the number of crossings of edges is even or odd.
(2) the product of u for each solid edge.

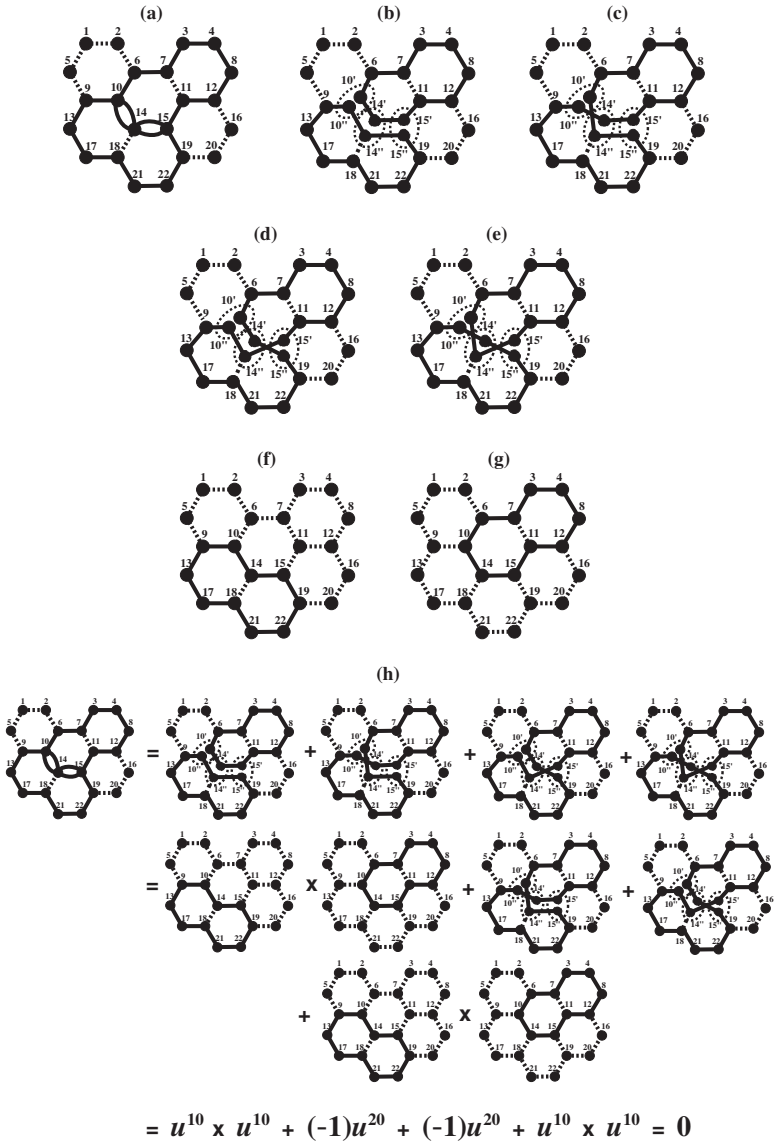

Fig. 6. An example of configurations including two double solid edges and their replacements. The contribution for configuration (a) is replaced by the sum of contributions (b)–(e). We see that there occur some crossings in (c) and (e). Both configurations in (b) and (e) consists of two cycles of solid edges in (f) and (g) and each contribution is the product of the contributions of (f) and (g). The contribution for configuration (a) is derived as shown in (h) and is equal to zero because a cycle of solid edges includes an additional factor $(-1)^r$ if there are r crossings in the cycle.

Thus, a cycle of solid edges includes an additional factor $(-1)^r$ if there are r crossings in the cycle. Some examples of configurations including double solid edges are shown in Figs. 5 and 6. In the configuration of Fig. 5(a), we have one double solid edge in $\{14, 15\}$. The vertices 14 and 15 in the double solid edge $\{14, 15\}$ are divided into vertices $14'$ and $14''$, and $15'$ and $15''$, respectively. One of the choices of the double solid edge on $\{14, 15\}$ is the pair $\{\{14', 15'\}, \{14'', 15''\}\}$ as shown in Fig. 5(b), and the other one is the pair $\{\{14', 15''\}, \{14'', 15'\}\}$ as shown in Fig. 5(c). We regard the configuration including two distinct cycles of solid edges in Fig. 5(b) as a product of two configurations including one cycle of solid edges as shown in Figs. 5(d) and (e). The contribution is given by the product of the contributions of Figs. 5(d) and (e). The contribution for configuration (a) is derived as shown in Fig. 5(f) and is equal to zero because the contribution of the cycle in Fig. 5(b) includes an additional factor -1 if there is one crossing in the cycle. Also for the example of Fig. 6(a), an argument similar to the above statements for the case of Fig. 5(a) holds. The contribution for Fig. 6(a) is rewritten as shown in Fig. 6(h) and is equal to zero because each contribution for Figs. 6(c) and (d) includes an additional factor $(-1)^r$ if there are r crossings in the cycle. Generally we have the following equality:

$$\{\text{every connected cycle that includes multiple solid edges}\} = 0. \tag{7}$$

Here the connected cycle is the configuration consisting of one cycle of solid edges. This cancellation of configurations expressed by the above equality (7), is due to the introduction of the additional factor $(-1)^r$ when r crossings occur in

cycles of solid edges [12]. By using Eq. (7), we obtain

$$\{\text{the sum of all the products of connected cycles that include multiple solid edges}\} = 0. \tag{8}$$

From these contributions, we have the following equality:

$$\begin{aligned}&\exp(\{\text{the sum of all the connected cycles that allow for multiple solid edges}\})\\ &= \sum_{n=0}^{+\infty} \frac{1}{n!} (\{\text{the sum of all the connected cycles that allow for multiple solid edges}\})^n\\ &= 1 + \{\text{the sum of all the products of connected cycles that allow for multiple solid edges}\}.\end{aligned} \tag{9}$$

By substituting Eq. (8) to Eq. (9) and by comparing it with Eq. (6), we derive the following equality:

$$Z(u) = \exp(\{\text{the sum of all the connected cycles that allow for multiple solid edges}\}). \tag{10}$$

Now we associate a direction to an undirected solid edge from one of the vertices i to the other $j(\in \partial i)$ and call such a directed edge a *step*. The number of possible steps starting with vertex i is $|\partial i|$. These steps are labeled as (i, μ) $(\mu = 1, 2, \cdots, |\partial i|)$, where i is the initial vertex of the step. If the initial vertex of the step (j, μ') is equal to the terminal vertex of the step (i, μ), step (j, μ') can follow (i, μ). By using these steps, we consider a random walk via these steps. A random walk via the steps returning to the initial vertex is called a directed cycle. A directed cycle is a cycle graph with all the solid edges being oriented in the same direction. Each undirected cycle of solid edges corresponds to two directed cycles consisting of the same solid edges, to which we associate the two opposite directions. The two directed cycles give the same contribution to the partition function. Eq. (10) can now be rewritten as

$$Z(u)^2 = \exp(\{\text{the sum of all the directed and connected cycles consisting of steps and allowing multiple steps}\}). \tag{11}$$

Now we introduce an $N\sum_{i\in V}|\partial i| \times N\sum_{i\in V}|\partial i|$ matrix $\mathbf{\Lambda}$ which indexes a random walk and has an element $\langle j, \mu'|\mathbf{\Lambda}|i, \mu\rangle$ for every pair of steps (i, μ) and (j, μ'). Its matrix elements are defined by

$$\langle j, \mu'|\mathbf{\Lambda}|i, \mu\rangle = u\eta(j, \mu' \mid i, \mu), \tag{12}$$

if the step (j, μ') can follow the step (i, μ), and it is zero otherwise.

To make the explicit calculations of the following section more understandable, we further discuss the matrix elements (12) by considering an undirected planar graph G which is embedded in the xy-plane. We denote the position vector of the vertex i by $\boldsymbol{R}_i$. Moreover we denote the position vector of the initial vertex of the step (i, μ) by $\boldsymbol{R}_{i,\mu}$. If (j, μ') can follow (i, μ), the initial vertex of the step (j, μ') is uniquely determined as the terminal vertex of (i, μ) and the step (i, μ) corresponds to the vector $\boldsymbol{R}_j - \boldsymbol{R}_i$. Hence $\boldsymbol{R}_{i,\mu}$ is defined by

$$\boldsymbol{R}_{i,\mu} \equiv \boldsymbol{R}_j - \boldsymbol{R}_i \ ((j, \mu') \text{ can follow } (i, \mu)). \tag{13}$$

We define that the value of $\eta(j, \mu' \mid i, \mu)$ is zero if $\boldsymbol{R}_{i,\mu} = -\boldsymbol{R}_{j,\mu'}$. When $\boldsymbol{R}_{i,\mu} \neq -\boldsymbol{R}_{j,\mu'}$, the value of $\eta(j, \mu' \mid i, \mu)$ is -1 if either of the following conditions (1) and (2) is satisfied, and the value is $+1$ otherwise.

(1) The vector $\boldsymbol{R}_{j,\mu'}$ whose y component is negative has a direction rotated clockwise less than π from the vector $\boldsymbol{R}_{i,\mu}$ whose y component is not negative [23].
(2) The vector $\boldsymbol{R}_{j,\mu'}$ whose y component is not negative has a direction rotated counter-clockwise less than π from the vector $\boldsymbol{R}_{i,\mu}$ whose y component is negative [23].

In terms of the matrix $\mathbf{\Lambda}$, we have the following equality:

$$\{\text{the sum of all the directed cycles consisting of } n \text{ steps}\} = -\frac{1}{n}\operatorname{Tr}\mathbf{\Lambda}^n. \tag{14}$$

By substituting Eq. (14) to Eq. (11), we can express the partition function as

$$Z(u)^2 = \exp\left(-\sum_{n=1}^{+\infty}\frac{1}{n}\operatorname{Tr}\mathbf{\Lambda}^n\right) = \det(\boldsymbol{I} - \mathbf{\Lambda}). \tag{15}$$

Here $\boldsymbol{I}$ is the $N\sum_{i\in V}|\partial i| \times N\sum_{i\in V}|\partial i|$ identity matrix. The detailed proof has been given in Secs. 2 and 3 in [11, 12]. Note that $\mathbf{\Lambda}$ is only dependent on the topological properties of the graph and can be defined intrinsically without any reference to an embedding of the corresponding graph in $\mathbb{R}^2$.

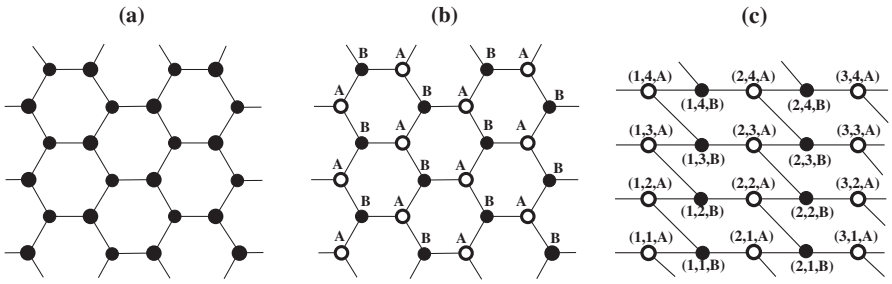

Fig. 7. An example of regular graphs.

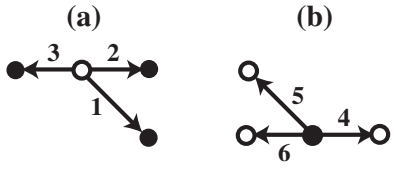

Fig. 8. Number of each step for the regular graph in Fig. 7.

We see that the free energy $F \equiv -\ln(Z(u))$ of the present system is expressed as

$$F = -\frac{1}{2}\ln(\det(\boldsymbol{I} - \boldsymbol{\Lambda})). \tag{16}$$

By substituting Eq. (4) to Eq. (15), we have the following equality:

$$\begin{aligned}\frac{1}{|E|}\sum_{\{i,j\}\in E}\Pr\{S_{ij} = 1 \mid u\} &= \frac{1}{u|E|}\frac{\partial}{\partial u}\left(\frac{1}{2}\ln(\det(\boldsymbol{I} - \boldsymbol{\Lambda}))\right) \\ &= \frac{1}{2u|E|}\mathrm{Tr}\left((\boldsymbol{I} - \boldsymbol{\Lambda})^{-1}\frac{\partial}{\partial u}(\boldsymbol{I} - \boldsymbol{\Lambda})\right).\end{aligned} \tag{17}$$

Note that both the expressions (16) and (17) are independent of any particular embedding, just as $\boldsymbol{\Lambda}$ is.

In the present section, we have given the derivation of the partition function $Z(u)$ in Eq. (2) by using the diagrammatical method. We remark again that the probabilistic model is defined on a planar graph such that the degree of every vertex is either two or three. By differentiating the partition function with respect to $\ln(u)$, we can obtain the value of the average of the marginal probabilities of the random variable S_{ij} considering all the edges $\{i, j\}(\in E)$, i.e. $\frac{1}{|E|}\sum_{\{i,j\}\in E}\Pr\{S_{ij} = 1 \mid u\}$.

4. Expression for the Honeycomb Lattice

We consider a regular graph as the one given in Fig. 7(a). The regular graph has periodic boundary conditions for the horizontal and the vertical directions in the plane. All vertices of the regular graph can be divided into two kinds of subgraphs A and B as shown in Fig. 7(b). Moreover, the regular graph in Fig. 7(b) is isomorphic to the one in Fig. 7(c). In Fig. 7(c), the vertices are labeled by (x, y, n) $(x = 1, 2, \ldots, K;\ y = 1, 2, \ldots, L;\ n = \mathrm{A}, \mathrm{B})$, where x and y denote the positions along the (horizontal) x-direction and the (vertical) y-direction, respectively, and n denotes the species of the subgraphs. The total number of vertices is $2KL$, and the total number of unit cells is KL.

There are six steps whose initial vertices are in the same unit cell. The steps are labeled by $\mu(= 1, 2, \ldots, 6)$. The way we label them is explicitly presented in Fig. 8. Due to translational symmetry for the edges, if a step $((1, 1), \mu)$ is the one from $(1, 1, n)$ to (x', y', n'), we also have a step $((x, y), \mu)$ from (x, y, n) to $(x' + x - 1, y' + y - 1, n')$. In this way, all steps can be labeled by $((x, y), \mu)$ $(x = 1, 2, \ldots, K;\ y = 1, 2, \ldots, L)$. The position vector $\boldsymbol{R}_{(x,y),\mu}$ of the initial vertex of step $((x, y), \mu)$ can be expressed as

$$\begin{aligned}\boldsymbol{R}_{(x,y),\mu} &= (2x - \delta_{\mu,1} - \delta_{\mu,2} - \delta_{\mu,3})\boldsymbol{e}_x + y\boldsymbol{e}_y, \\ &\quad (x = 1, 2, \ldots, K; y = 1, 2, \ldots, L),\end{aligned} \tag{18}$$

where $\boldsymbol{e}_x$ and $\boldsymbol{e}_y$ are the unit vectors in the x-direction and the y-direction, respectively. The vector $\boldsymbol{R}_\mu$ of Fig. 8, are explicitly given by

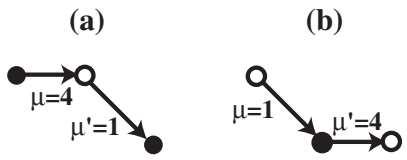

Fig. 9. Combination of steps that give $\eta(j,\mu' \mid i,\mu) = -1$ when the step (j,μ') follows the step (i,μ) for the regular graph of Fig. 7.

$$\begin{cases} \boldsymbol{R}_1 = \boldsymbol{e}_x - \boldsymbol{e}_y, & \boldsymbol{R}_2 = \boldsymbol{e}_x, & \boldsymbol{R}_3 = -\boldsymbol{e}_x, \\ \boldsymbol{R}_4 = \boldsymbol{e}_x, & \boldsymbol{R}_5 = -\boldsymbol{e}_x + \boldsymbol{e}_y, & \boldsymbol{R}_6 = -\boldsymbol{e}_x. \end{cases} \tag{19}$$

Pairs of μ and μ' for which the value of $\eta_{\mu,\mu'}$ is -1 are shown in Fig. 9. The value of $\eta_{\mu,\mu'}$ for the other pairs is zero or unity.

Now we consider wave number vectors

$$\boldsymbol{Q}_{p,q} = \frac{\pi p}{K}\boldsymbol{e}_x + \frac{2\pi q}{L}\boldsymbol{e}_y, \tag{20}$$

and introduce a $6KL \times 6KL$ matrix $\boldsymbol{\Psi}$ defined by

$$\langle x,y,\mu|\boldsymbol{\Psi}|p,q,\mu'\rangle \equiv \frac{1}{\sqrt{KL}} e^{-i\boldsymbol{R}_{(x,y),\mu}\cdot\boldsymbol{Q}_{p,q}}\delta_{\mu,\mu'}. \tag{21}$$

We have the inverse matrix $\boldsymbol{\Psi}^{-1}$ as follows:

$$\langle p,q,\mu'|\boldsymbol{\Psi}^{-1}|x,y,\mu\rangle \equiv \frac{1}{\sqrt{KL}} e^{i\boldsymbol{Q}_{p,q}\cdot\boldsymbol{R}_{(x,y),\mu}}\delta_{\mu,\mu'}. \tag{22}$$

We introduce a discrete Fourier transformation of $\boldsymbol{I} - \boldsymbol{\Lambda}$ as follows:

$$\boldsymbol{I} - \widehat{\boldsymbol{\Lambda}} \equiv \boldsymbol{\Psi}^{-1}(\boldsymbol{I} - \boldsymbol{\Lambda})\boldsymbol{\Psi} \tag{23}$$

$$\boldsymbol{I} - \boldsymbol{\Lambda} \equiv \boldsymbol{\Psi}(\boldsymbol{I} - \widehat{\boldsymbol{\Lambda}})\boldsymbol{\Psi}^{-1} \tag{24}$$

When the step $((x',y'),\mu')$ follows the step $((x,y),\mu)$, the vector $\boldsymbol{r}_{(x,y),\mu}$ for the step $((x,y),\mu)$ is defined by

$$\boldsymbol{r}_\mu \equiv \boldsymbol{R}_{(x',y'),\mu'} - \boldsymbol{R}_{(1,1),\mu}. \tag{25}$$

If the step $((x',y'),\mu')$ follows the step $((1,1),\mu)$, the step $((x'+x-1,y'+y-1),\mu')$ also follows the step $((x,y),\mu)$ because of the translational symmetry for edges. When the step $((x'+x-1,y'+y-1),\mu')$ follows the step $((x,y),\mu)$, we introduce the vector $\boldsymbol{r}_{(x,y),\mu}$ for the step $((x,y),\mu)$ which is defined by

$$\boldsymbol{r}_{(x,y),\mu} = \boldsymbol{R}_{(x'+x-1,y'+y-1),\mu'} - \boldsymbol{R}_{(x,y),\mu}. \tag{26}$$

The vector $\boldsymbol{r}_{(x,y),\mu}$ does not depends on (x,y) and we can replace the vector $\boldsymbol{r}_{(x,y),\mu}$ by a notation $\boldsymbol{r}_\mu$ in the present case. The matrix $\boldsymbol{I} - \widehat{\boldsymbol{\Lambda}}$ can be rewritten as

$$\begin{aligned} \langle p,q,\mu|\boldsymbol{I} - \widehat{\boldsymbol{\Lambda}}|p',q',\mu'\rangle &= \frac{1}{KL}\sum_{x=1}^{K}\sum_{y=1}^{L}\sum_{x'=1}^{K}\sum_{y'=1}^{L}\langle x,y,\mu|\boldsymbol{I} - \boldsymbol{\Lambda}|x',y',\mu'\rangle \\ &\quad \times e^{i\boldsymbol{Q}_{p,q}\cdot\boldsymbol{r}_{\mu'} + i(\boldsymbol{Q}_{p,q} - \boldsymbol{Q}_{p',q'})\cdot\boldsymbol{R}_{(x',y'),\mu'}} \\ &= \frac{1}{KL}\{\delta_{\mu,\mu'} - u\eta_{\mu,\mu'}e^{i\boldsymbol{Q}_{p,q}\cdot\boldsymbol{r}_{\mu'}}\}\sum_{x'=1}^{K}\sum_{y'=1}^{L} e^{i(\boldsymbol{Q}_{p,q} - \boldsymbol{Q}_{p',q'})\cdot\boldsymbol{R}_{(x',y'),\mu'}} \\ &= \delta_{p,p'}\delta_{q,q'}\{\delta_{\mu,\mu'} - u\eta_{\mu,\mu'}e^{i\boldsymbol{Q}_{p,q}\cdot\boldsymbol{r}_{\mu'}}\}. \end{aligned} \tag{27}$$

By substituting Eq. (27) to Eq. (15), we obtain

$$Z(u)^2 = \prod_{p=1}^{K}\prod_{q=1}^{L}\det\left(\boldsymbol{I} - \boldsymbol{A}\left(\frac{2\pi p}{K},\frac{2\pi q}{L}\right)\right) \tag{28}$$

$$\langle\mu|\boldsymbol{A}\left(\frac{2\pi p}{K},\frac{2\pi q}{L}\right)|\mu'\rangle \equiv u\eta_{\mu,\mu'}e^{i\boldsymbol{Q}_{p,q}\cdot\boldsymbol{r}_{\mu'}}. \tag{29}$$

such that,

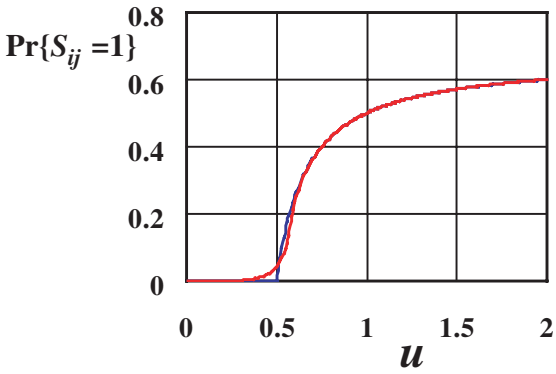

Fig. 10. Marginal Probability $\Pr\{S_{ij} = 1 \mid u\}$ for the regular graph in Fig. 7. The red line is an exact result obtained by using the diagrammatical method. The blue line is an approximate result obtained by using the loopy belief propagation (LBP).

$$\boldsymbol{A}(\theta,\phi) = \begin{pmatrix} 0 & 0 & 0 & -ue^{i\theta/2} & 0 & ue^{-i\theta/2} \\ 0 & 0 & 0 & ue^{i\theta/2} & ue^{-i(\theta/2-\phi)} & 0 \\ 0 & 0 & 0 & 0 & ue^{-i(\theta/2-\phi)} & ue^{-i\theta/2} \\ -ue^{i(\theta/2-\phi)} & ue^{i\theta/2} & 0 & 0 & 0 & 0 \\ 0 & ue^{i\theta/2} & ue^{-i\theta/2} & 0 & 0 & 0 \\ ue^{i(\theta/2-\phi)} & 0 & ue^{-i\theta/2} & 0 & 0 & 0 \end{pmatrix} \tag{30}$$

The free energy $f(u)$ per unit cell in the thermodynamic limit is given as follows:

$$\begin{aligned} f(u) &\equiv -\lim_{K\to+\infty}\lim_{L\to+\infty}\frac{1}{KL}\ln(Z(u)) \\ &= -\frac{1}{8\pi^2}\int_{-\pi}^{+\pi}\int_{-\pi}^{+\pi}\ln(\det(\boldsymbol{I}-\boldsymbol{A}(\theta,\phi)))d\theta d\phi \\ &= -\frac{1}{8\pi^2}\int_{-\pi}^{+\pi}\int_{-\pi}^{+\pi}\ln\Bigg(1+3u^4-2u^2(1-u^2)\cos(\phi) \\ &\qquad -4u^2(1-u^2)\cos\left(\frac{\phi}{2}\right)\cos\left(2\theta+\frac{\phi}{2}\right)\Bigg)d\theta d\phi. \end{aligned} \tag{31}$$

This result is consistent with the one given in Ref. [8].

Due to the translational symmetry and the periodic boundary condition of the system considered in the present section, the marginal probability $\Pr\{S_{ij} = 1 \mid u\}$ does not depend on the edge $\{i, j\}$. By using Eq. (17) and Eq. (31), the marginal probability $\Pr\{S_{ij} = 1 \mid u\}$ can be derived as follows:

$$\begin{aligned} \Pr\{S_{ij} = 1 \mid u\} &= -\left(\frac{u}{3}\right)\frac{\partial}{\partial u}f(u) \\ &= \frac{1}{6\pi^2}\int_{-\pi}^{+\pi}\int_{-\pi}^{+\pi}\frac{3u^4-u^2(1-2u^2)\cos(\phi)-2u^2(1-2u^2)\cos(\frac{\phi}{2})\cos(2\theta+\frac{\phi}{2})}{1+3u^4-2u^2(1-u^2)\cos(\phi)-4u^2(1-u^2)\cos(\frac{\phi}{2})\cos(2\theta+\frac{\phi}{2})}d\theta d\phi. \end{aligned} \tag{32}$$

The integrals in Eqs. (31) and (32) are improper integrals when $u = 1/\sqrt{3}$. The numerator of integrand in Eq. (32) satisfies the following inequalities:

$$\begin{aligned} &1+3u^4-2u^2(1-u^2)\cos(\phi)-4u^2(1-u^2)\cos\left(\frac{\phi}{2}\right)\cos\left(2\theta+\frac{\phi}{2}\right) \\ &\quad = 1+3u^4-2u^2(1-u^2)(\cos(\phi)+\cos(\theta)+\cos(2\theta+\phi)) \\ &\quad \geq \begin{cases} (1-3u^2)^2 & (0<u\leq 1) \\ (1+u^2)^2 & (u\geq 1) \end{cases}. \end{aligned} \tag{33}$$

The denominator $1+3u^4-2u^2(1-u^2)\cos(\phi)-4u^2(1-u^2)\cos(\frac{\phi}{2})\cos(2\theta+\frac{\phi}{2})$ of the integrand in Eq. (32) does not vanish for any real numbers of θ and ϕ except in the case of $u = 1/\sqrt{3}$. The denominator of the integrand is equal to zero only at $\theta = \phi = 0$ in the case of $u = 1/\sqrt{3}$ and the integrand diverges only at that point. Thus, the integral in Eq. (32) can be regarded as an improper integral when $u = 1/\sqrt{3}$.

Though the values of $\Pr\{S_{ij} = 1 \mid u\}$ take finite values, its derivative $\frac{\partial}{\partial u}\Pr\{S_{ij} = 1 \mid u\}$ diverges for $u = 1/\sqrt{3}$. It means that a phase transition occurs at $u = 1/\sqrt{3}$. Moreover we see that $\lim_{u\to+\infty}\Pr\{S_{ij} = 1 \mid u\} = 2/3$. The marginal probability $\Pr\{S_{ij} = 1 \mid u\}$ of Eq. (32) is shown in Fig. 10.

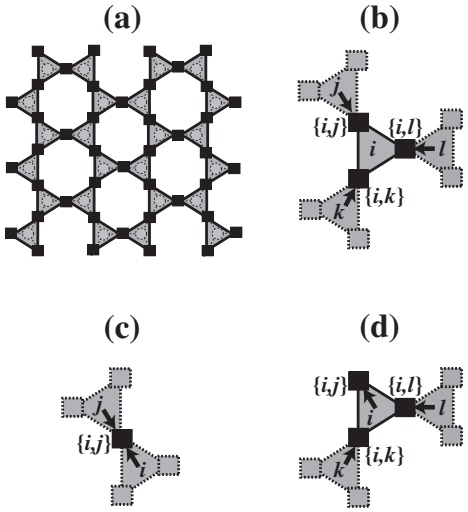

Fig. 11. Loopy belief propagation (LBP) of regular graphs. (a) Probabilistic model for cycles on the honeycomb lattice. (b) Graphical Representation for the marginal probability $\Pr\{S_{ij}, S_{ik}, S_{il}\}$ in LBP. (c) Graphical Representation for the marginal probability $\Pr\{S_{ij}\}$ in LBP. (d) Graphical Representation for the message passing rule in LBP.

5. Loopy Belief Propagation

In this section, we give an approximate calculation of the marginal probability $\Pr\{S_{ij} = 1 \mid u\}$ for the probabilistic model given in Sec. 2 defined on the honeycomb lattice obtained by means of LBP [24–26]. The graphical representation of the probabilistic model of Eq. (1) is given in Fig. 11(a).

In LBP, the marginal probability $\Pr\{S_{ij}, S_{ik}, S_{il}\}$ for the set of edges of which vertex i is an ending vertex and belongs to the set $V \backslash \partial V$, such that $|\partial i| = 3$, is approximated by the following expression

$$\begin{aligned}&\Pr\{S_{ij} = s, S_{ik} = s', S_{il} = s''\}\\ &\simeq \frac{u^{\frac{1}{2}(s+s'+s'')}(\delta_{s+s'+s'',0} + \delta_{s+s'+s'',2}) m_{j\to\{i,j\}}(s) m_{k\to\{i,k\}}(s') m_{l\to\{i,l\}}(s'')}{\sum_{s=0,1}\sum_{s'=0,1}\sum_{s''=0,1} u^{\frac{1}{2}(s+s'+s'')}(\delta_{s+s'+s'',0} + \delta_{s+s'+s'',2}) m_{j\to\{i,j\}}(s) m_{k\to\{i,k\}}(s') m_{l\to\{i,l\}}(s'')}.\end{aligned} \tag{34}$$

Similarly, the marginal probability $\Pr\{S_{ij}\}$ for edges $\{i, j\}$ of which i and j belong to the set $V \backslash \partial V$ is approximated by

$$\Pr\{S_{ij} = s\} \simeq \frac{m_{i\to\{i,j\}}(s) m_{j\to\{i,j\}}(s)}{\sum_{s=0,1} m_{i\to\{i,j\}}(s) m_{j\to\{i,j\}}(s)}. \tag{35}$$

Fig. 11(b) and (c) show the corresponding graphical representation of Eqs. (34) and (35), respectively.

Demanding consistency between all Eqs. (34) and (35), i.e.,

$$\Pr\{S_{ij} = s\} = \sum_{s'=0,1}\sum_{s''=0,1} \Pr\{S_{ij} = s, S_{ik} = s', S_{il} = s''\}, \tag{36}$$

we obtain the following update rule for the messages $\{m_{i\to\{i,j\}}(s), s = 0, 1\}$:

$$m_{i\to\{i,j\}}(s) = \frac{Z_{ij}}{Z_i}\sum_{s'=0,1}\sum_{s''=0,1} u^{\frac{1}{2}(s+s'+s'')}(\delta_{s+s'+s'',0} + \delta_{s+s'+s'',2}) m_{k\to\{i,k\}}(s') m_{l\to\{i,l\}}(s''). \tag{37}$$

Eq. (37) can be expressed in terms of the graphical representations in Fig. 11(d). If we now define a new normalized message

$$\lambda_{i\to\{i,j\}}(s) \equiv \frac{m_{i\to\{i,j\}}(s)}{\sum_{s=0,1} m_{i\to\{i,j\}}(s)}, \tag{38}$$

we can rewrite the edge marginals of Eq. (35) as following

$$\Pr\{S_{ij} = s\} \simeq \frac{\lambda_{i\to\{i,j\}}(s)\lambda_{j\to\{i,j\}}(s)}{\sum_{s=0,1}\lambda_{i\to\{i,j\}}(s)\lambda_{j\to\{i,j\}}(s)}. \tag{39}$$

By substituting Eq. (37) to the right-hand side of Eq. (38), we find the following update rule for the newly defined messages

$$\lambda_{i\to\{i,j\}}(s)=\frac{\sum_{s'=0,1}\sum_{s''=0,1}u^{\frac{1}{2}(s+s'+s'')}(\delta_{s+s'+s'',0}+\delta_{s+s'+s'',2})\lambda_{k\to\{i,k\}}(s')\lambda_{l\to\{i,l\}}(s'')}{\sum_{s=0,1}\sum_{s'=0,1}\sum_{s''=0,1}u^{\frac{1}{2}(s+s'+s'')}(\delta_{s+s'+s'',0}+\delta_{s+s'+s'',2})\lambda_{k\to\{i,k\}}(s')\lambda_{l\to\{i,l\}}(s'')}$$
$$(i\in V\backslash\partial V). \tag{40}$$

Eqs. (39) and (40) are illustrated in terms of the graphical representations in Fig. 11(b) and (d), respectively.

When the vertex i belongs to the set ∂V, the degree $|\partial i|$ of vertex i is two. In this case, Eq. (40) becomes

$$\lambda_{i\to\{i,j\}}(s)=\frac{\sum_{s'=0,1}u^{\frac{1}{2}(s+s')}(\delta_{s+s',0}+\delta_{s+s',2})\lambda_{k\to\{i,k\}}(s')}{\sum_{s=0,1}\sum_{s'=0,1}u^{\frac{1}{2}(s+s')}(\delta_{s+s',0}+\delta_{s+s',2})\lambda_{k\to\{i,k\}}(s')}\quad(i\in\partial V). \tag{41}$$

Due to the periodic boundary condition and the translational symmetry of the honeycomb lattice, the messages $\lambda_{i\to\{i,j\}}(s)$ are the same for all edges $\{i,j\}$. Moreover, as the state variables s_{ij} can take on only two values, they can be parametrized by a single message. We choose to denote the messages as λ when $s=1$. Thus, Eqs. (39) and (40) can be rewritten as follows:

$$\Pr\{S_{ij}=1\mid u\}\simeq\frac{\lambda^2}{(1-\lambda)^2+\lambda^2}, \tag{42}$$
$$\lambda=\frac{2u\lambda(1-\lambda)}{(1-\lambda)^2+u\lambda^2+2u\lambda(1-\lambda)} \tag{43}$$

By resolving Eq. (43) for λ, we obtain

$$\lambda=\frac{(1-2u)+\sqrt{u(2u-1)}}{1-u}. \tag{44}$$

The messages λ thus have a singularity for $u=1$, where it takes on the value $\lim_{u\to1}\lambda=1/2$.

By substituting Eq. (43) into Eq. (42), we obtain

$$\Pr\{S_{ij}=1\mid u\}\simeq\begin{cases}0 & (u<\frac{1}{2})\\ \dfrac{2u-1}{3u-1} & (u>\frac{1}{2})\end{cases}. \tag{45}$$

The marginal probability $\Pr\{S_{ij}=1\mid u\}$ of Eq. (45) is shown in Fig. 10. In the result obtained by means of LBP, we see that a phase transition occurs at $u=1/2$, which is earlier than the exact result $u=1/\sqrt{3}$. Instead, the LBP result for $\lim_{u\to+\infty}\Pr\{S_{ij}=1\mid u\}=2/3$ coincides with the exact limit.

6. Numerical Experiments for Finite Planar Graphs

In this section, we give some numerical results for the finite planar graphs shown in Fig. 12, which have no periodic boundary conditions. We check the difference between the results for $\frac{1}{|E|}\sum_{\{i,j\}\in E}\Pr\{S_{ij}=1\mid u\}$ obtained by means of the diagrammatical method and LBP for each planar graph. Note that the equalities (16) and (17) are valid for finite planar graphs.

In the exact diagrammatical method given in Sec. 3, we have to generate the matrix $\mathbf{\Lambda}$ defined by Eq. (12) for each planar graph. For the finite planar graph of Fig. 12(a), we show all the elements of the matrix $\mathbf{\Lambda}$ explicitly in Fig. 13. The exact results for $\frac{1}{|E|}\sum_{\{i,j\}\in E}\Pr\{S_{ij}=1\mid u\}$ by the diagrammatical method are obtained by using Eq. (17). The LBP approximation for the average of the marginals $\frac{1}{|E|}\sum_{\{i,j\}\in E}\Pr\{S_{ij}=1\mid u\}$ are obtained from the value of the messages (40) at their fixed point according to Eq. (39). The obtained results of $\frac{1}{|E|}\sum_{\{i,j\}\in E}\Pr\{S_{ij}=1\mid u\}$ for each regular graph of Figs. 12(a)–(c) are shown in Fig. 14. The red curves are the exact results obtained by using the diagrammatical method, whereas the blue curves are the LBP results.

In Figs. 15 and 16, we explicitly show the size dependence of $\frac{1}{|E|}\sum_{\{i,j\}\in E}\Pr\{S_{ij}=1\mid u\}$ according to the diagrammatical method and LBP, respectively. We see that the results converge systematically to the one for the infinite planar graph given in Fig. 7. It is interesting to note that $u=1$ signals a crossover point for both methods. For $u<1$, the edge marginals $\Pr\{S_{ij}=1\mid u\}$ are, on average, lower for smaller graphs. Instead, for $u>1$, the results for $\frac{1}{|E|}\sum_{\{i,j\}\in E}\Pr\{S_{ij}=1\mid u\}$ on finite graphs overestimate the case of the infinite graph, and more so for smaller graphs. More specifically, there exist large differences between the LBP results and the exact ones obtained using the diagrammatical method in the region for u near the transition point of the present model on the infinite planar graph, i.e., $u=1/2$ and $u=1/\sqrt{3}$, respectively. For all the infinite and finite graphs presented in Figs. 7 and 12, $\frac{1}{|E|}\sum_{\{i,j\}\in E}\Pr\{S_{ij}=1\mid u\}$ is always equal to $1/2$ for $u=1$.

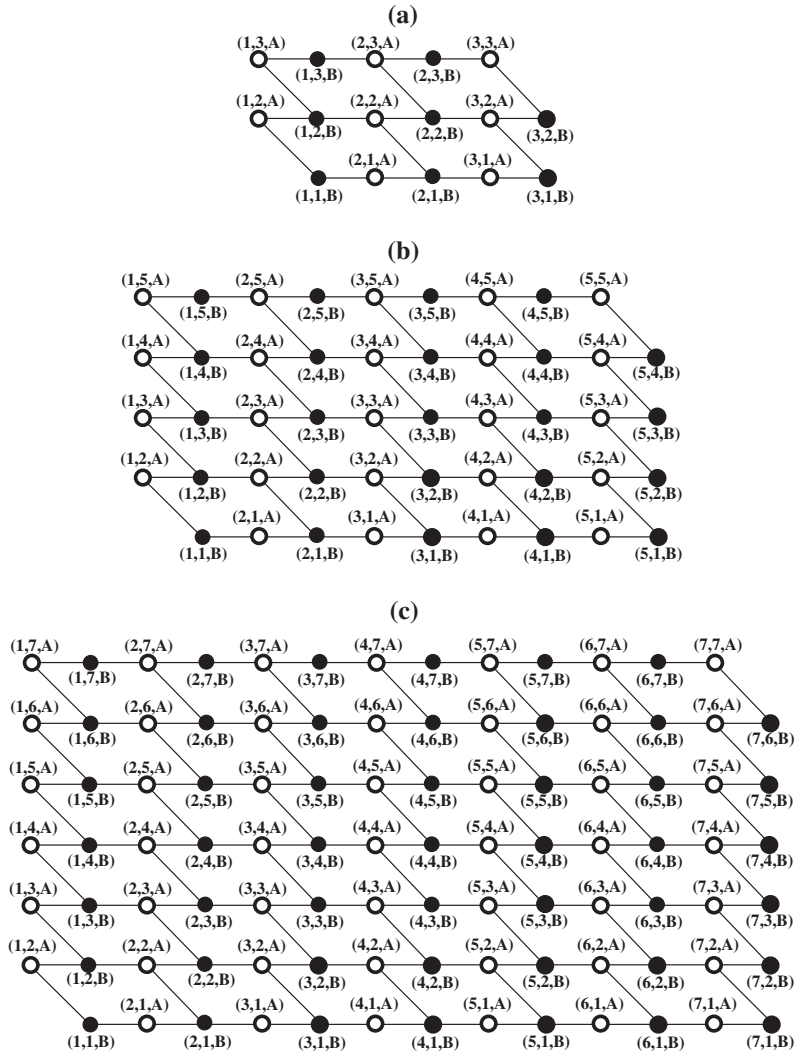

Fig. 12. Finite planar graphs. (a) $K = L = 3$, $|V| = 16$, $|E| = 19$. (b) $K = L = 5$, $|V| = 48$, $|E| = 63$. (c) $K = L = 7$, $|V| = 96$, $|E| = 131$.

Figs. 14(a)–(c) present comparative results according to the two methods for the finite graphs of Fig. 12. It is clear that for $u > 1$ LBP delivers good approximate values with respect to the exact solution for $\frac{1}{|E|}\sum_{\{i,j\}\in E}\Pr\{S_{ij} = 1 \mid u\}$. However, for lower values, i.e., $u < 1$, we find LBP sometimes overestimates, sometimes underestimates the exact results.

To understand the above behaviour better, we present in Figs. 17(a)–(b) the full distribution of $\Pr\{S_{ij} = 1 \mid u\}$ for some value of $u < 1$ and $u > 1$, respectively. The step function character is more explicit for larger systems as these are less prone to finite size effects. While for $u < 1$ none of the edges have a marginal larger than the typical value, for $u > 1$ some do. From Fig. 18 it is clear that the LBP estimation of the marginals of the outer edges which have at least one ending vertex of degree 2, overestimates the overall expected typical value.

7. Perturbative Analysis near $u = 1$

In this section, we discuss the asymptotic behaviour of $\Pr\{S_{ij} = 1 \mid u\}$ near $u = 1$ such that $\ln(u) = 0$. The regions $0 < u < 1$ and $u > 1$ correspond to $\ln(u) < 0$ and $\ln(u) > 0$, respectively. Since we have $u^{S_{ij}} = \exp(S_{ij}\ln(u))$, $\ln(u)$ can be regarded as a chemical potential conjugated to the number of solid edges. In this section, we give some perturbative calculations in the case of infinitesimal $\ln(u)$.

First we consider a dual graph $G^* = (V^*, E^*)$ for each finite planar graph $G = (V, E)$. Here V^* and E^* are the sets of vertices and edges in the dual graph G^*, respectively. The number of elements of the set E^*, i.e. $|E^*|$, is equal to the number of edges $|E|$ of the original graph $G = (V, E)$. If we denote the set of vertices for which the degree is two in the graph $G = (V, E)$ by ∂V, we now introduce an additional set of edges ∂E^* for which we demand that $|\partial E^*| = |\partial V|$. For example, the dual graph of the planar graph in Fig. 12(b) is shown as Fig. 19(a). If both $\{i, j\}$ and $\{j, k\}$ belong to E^* but $\{i, k\}$ does not belong to E^*, we regard $\{i, k\}$ as an additional edge. In the dual graph $G^* = (V^*, E^*)$, there exist some

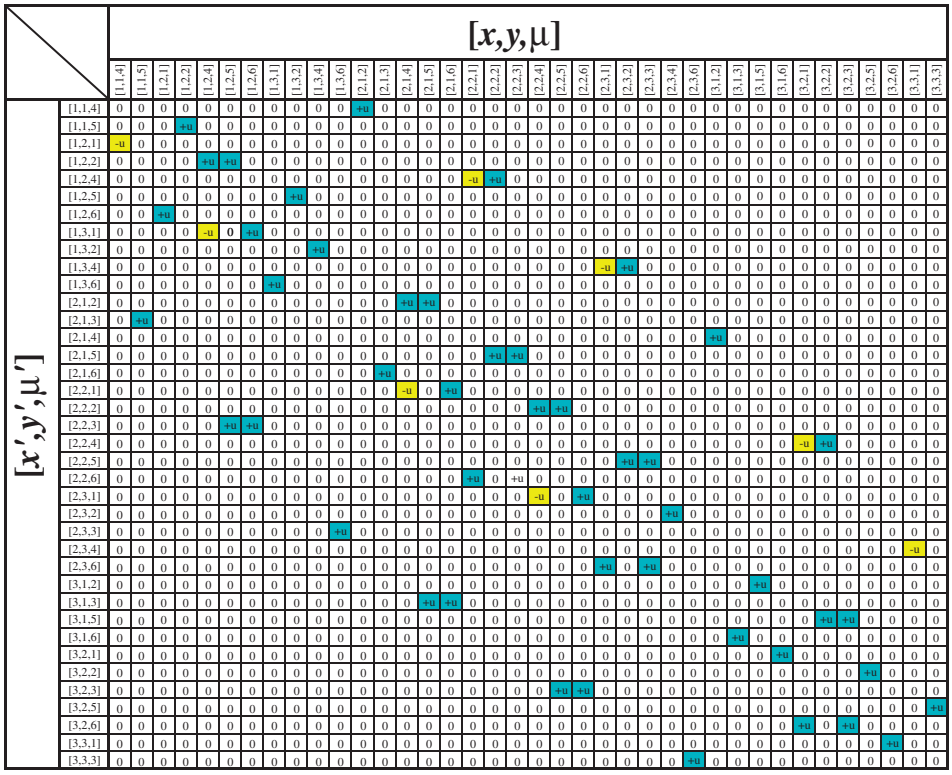

Fig. 13. Matrix $\mathbf{\Lambda}$ of the finite regular graph in Fig. 12(a).

vertices of degree one. The set of all the vertices of which the degree is one is denoted by $\partial V^* \equiv \{i \mid |\partial i| = 1\}$. We introduce additional edges $\{i, j\}$ for some pairs of vertices, i and j, belonging to ∂V^* in the dual graph $G^* = (V^*, E^*)$. The set of such additional edges are denoted by the notation ∂E^*. The set ∂E^* has been chosen such that the graph $(V^*, E^* + \partial E^*)$ is also a planar graph and $|\partial i| = 3$ for any vertices i belonging to ∂V^*. For example, we can introduce ∂E^* for the planar dual graph $G^* = (V^*, E^*)$ in Fig. 19(a) as shown in Fig. 19(b).

We assign a spin variable $\sigma_i (= \pm 1)$ to each vertex $i \in V^*$ in the dual graph G^*. In terms of the dual graph G^* and the set of additional edges ∂E^*, the partition function $Z(u)$ in Eq. (2) are rewritten as follows:

$$Z(u) = \frac{1}{2} \sum_{\boldsymbol{\sigma}} \left(\prod_{\{i,j\} \in E^*} u^{-\frac{1}{2}(\ln(u))(\sigma_i \sigma_j - 1)} \right) \left(\prod_{\{i,j\} \in \partial E^*} \delta_{\sigma_i \sigma_j, 1} \right) \tag{46}$$

The summation $\sum_{\boldsymbol{\sigma}} \equiv \sum_{\{\sigma_i = \pm 1 | i \in V^*\}}$ is taken with respect to all the spin variables for vertices in the set V^*. Since we have $\delta_{\sigma_i \sigma_j, 1} = \frac{1}{2}(1 - \sigma_i \sigma_j)$ and $u^{-\frac{1}{2}(\sigma_i \sigma_j - 1)} = \cosh(\frac{1}{2}\ln(u)) - \sinh(\frac{1}{2}\ln(u))\sigma_i \sigma_j$, the logarithm of partition function $Z(u)$ can be given as a series of $\tanh^2(\frac{1}{2}\ln(u))$:

$$\begin{aligned}
\ln Z(u) &= \ln\left(\frac{1}{2}\right) + |E^*| \ln\left(\cosh\left(\frac{1}{2}u\right)\right) + |\partial E^*| \ln\left(\frac{1}{2}\right) \\
&\quad + \ln\left\{ \sum_{\boldsymbol{\sigma}} \left(\prod_{\{i,j\} \in E^*} \left(1 - \tanh\left(\frac{1}{2}\ln(u)\right)\sigma_i \sigma_j\right)\right) \left(\prod_{\{i,j\} \in \partial E^*} (1 + \sigma_i \sigma_j) \right) \right\} \\
&= \ln\left(\frac{1}{2}\right) + |E^*| \ln\left(\cosh\left(\frac{1}{2}u\right)\right) + |\partial E^*| \ln\left(\frac{1}{2}\right) \\
&\quad + \ln\left(1 + |\partial E^*| \tanh^2\left(\frac{1}{2}\ln(u)\right) - |E^*| \tanh^3\left(\frac{1}{2}\ln(u)\right) + \cdots\right).
\end{aligned} \tag{47}$$

Here we use the equality $\sigma_i^2 = 1$ and $\sum_{\sigma_i = \pm 1} \sigma_i = 0$ in the derivation of the second equality. We derive the series expansion of $\frac{1}{|E|} \sum_{\{i,j\} \in E} \Pr\{S_{ij} = 1 \mid u\}$ with respect to $\tanh^2(\frac{1}{2}\ln(u))$ for infinitesimal $\ln(u)$ as follows:

$$\begin{aligned}
\frac{1}{|E|} \sum_{\{i,j\} \in E} \Pr\{S_{ij} = 1 \mid u\} &= \left(\frac{1}{u}\right) \frac{\partial}{\partial u} \ln Z(u) \\
&= \frac{1}{2} + \left(\frac{1}{2} + \frac{|\partial V|}{|E|}\right) \tanh\left(\frac{1}{2}\ln(u)\right) + \mathcal{O}\left(\tanh^2\left(\frac{1}{2}\ln(u)\right)\right) \ (u \to 1).
\end{aligned} \tag{48}$$

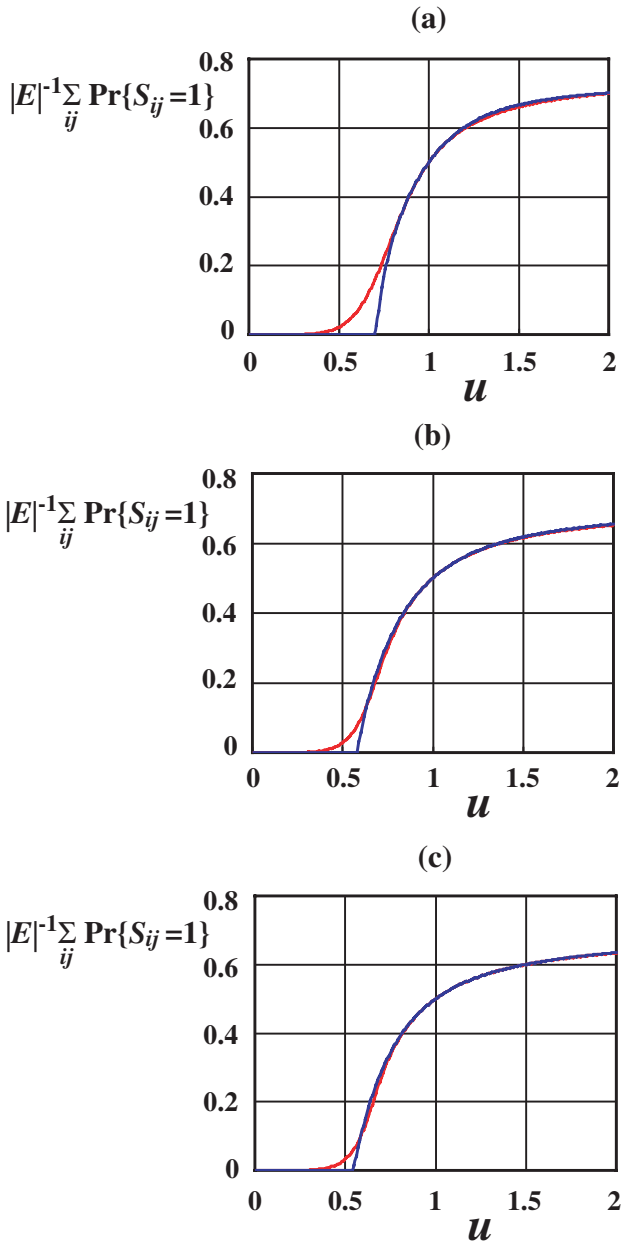

Fig. 14. Average of marginal probabilities over all the edges, $\frac{1}{|E|}\sum_{\{i,j\}\in E}\Pr\{S_{ij}=1 \mid u\}$, for each regular graph of Fig. 12. The red line is an exact result obtained by using the diagrammatical method. The blue line is an approximate result obtained by using the loopy belief propagation (LBP). (a) $K=L=3$, $|V|=16$, $|E|=19$. (b) $K=L=5$, $|V|=48$, $|E|=63$. (c) $K=L=7$, $|V|=96$, $|E|=131$.

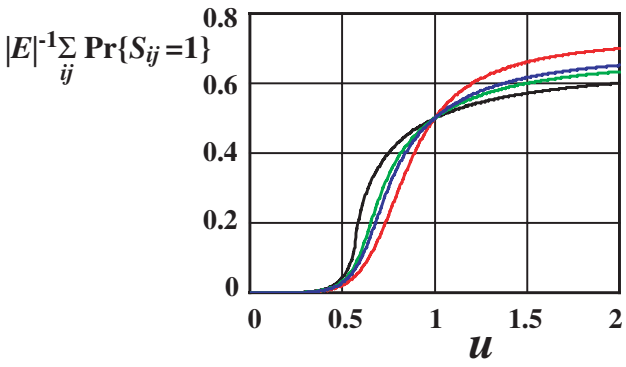

Fig. 15. Average of marginal probabilities over all the edges, $\frac{1}{|E|}\sum_{\{i,j\}\in E}\Pr\{S_{ij}=1 \mid u\}$, for each regular graph in Fig. 12. All lines are exact results obtained by using the diagrammatical method of Sec. 3. The black line is the result for the infinite planar graph in Fig. 7. The red, blue and green lines are for the finite planar graphs given in Figs. 12(a), 12(b) and 12(c), respectively.

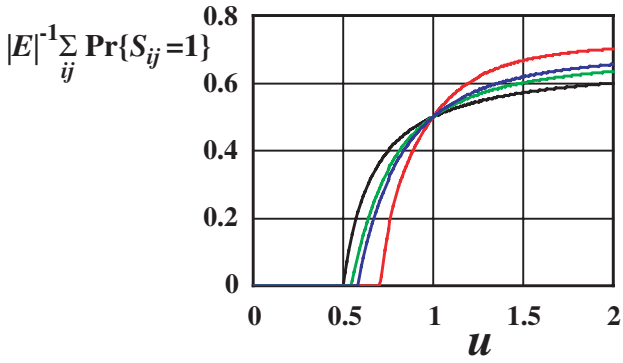

Fig. 16. Average of marginal probabilities over all the edges, $\frac{1}{|E|}\sum_{\{i,j\}\in E}\Pr\{S_{ij}=1 \mid u\}$, for each regular graph in Fig. 12. All lines are the approximate results obtained by using the LBP of Sec. 5. The black line is the result for the infinite planar graph given in Fig. 7. The red, blue and green lines are for the finite planar graphs in Figs. 12(a), 12(b) and 12(c), respectively.

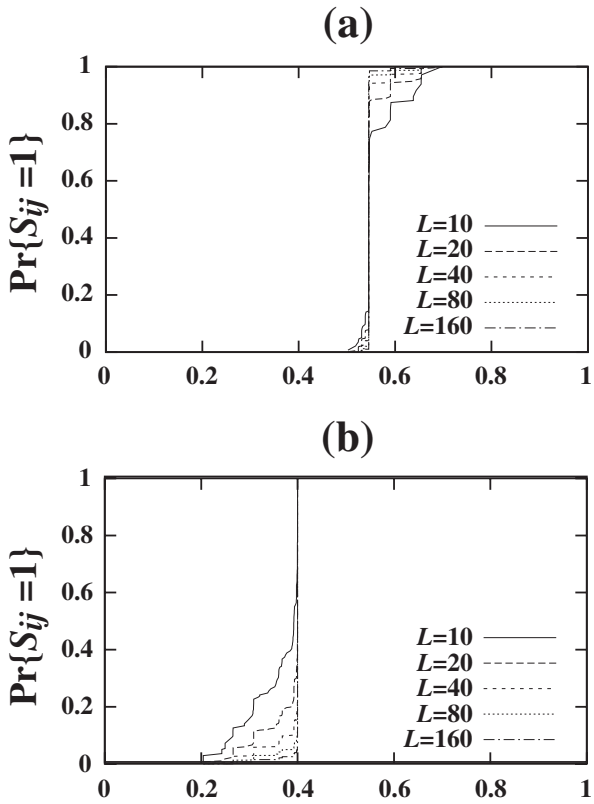

Fig. 17. Integrated distribution of the marginals $\Pr\{S_{ij}=1 \mid u\}$ for finite size honeycomb lattices of length $K=L=10,20,40,80,160$ for (a) $u=1.25$ and (b) $u=0.75$.

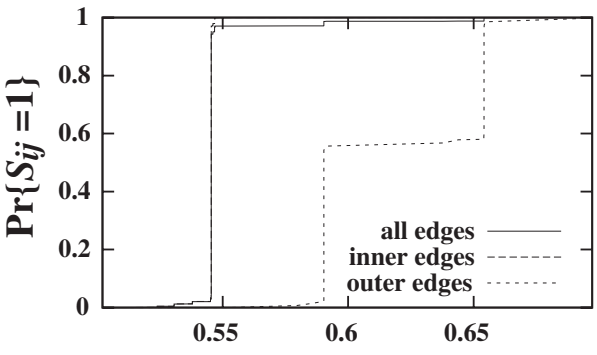

Fig. 18. Integrated distribution of $\Pr\{S_{ij}=1 \mid u\}$ considering either all edges, only the inner edges, or only the outer edges for the honeycomb lattice of $K=L=80$ for $u=1.25$.

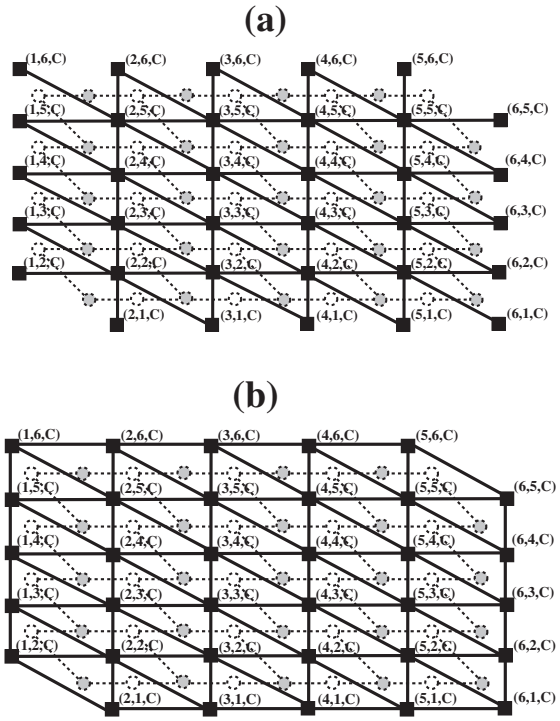

Fig. 19. Dual planar graph for the planar graph in Fig. 12(b). (a) $G^* = (V^*, E^*)$. (b) $(V^*, E^* + \partial E^*)$.

For $u = 1$, the average of the edge marginals $\frac{1}{|E|}\sum_{\{i,j\}\in E}\Pr\{S_{ij} = 1 \mid u\}$ is equal to $1/2$. In the case of infinitesimally positive $\ln(u)$, the average of marginals $\frac{1}{|E|}\sum_{\{i,j\}\in E}\Pr\{S_{ij} = 1 \mid u\}$ is larger than $1/2$ and increases when the ratio $|\partial V|/|E|$ increases. In the case of the infinitesimally negative $\ln(u)$, it is smaller than $1/2$ and decreases when the ratio $|\partial V|/|E|$ increases.

Secondly, if we consider the behaviour of the LBP at $u = 1$. Eqs. (40) and (41) have the solution $\lambda_{i\to\{i,j\}}(0) = \lambda_{i\to\{i,j\}}(1) = \frac{1}{2}$ ($\{i, j\} \in E$), which can be confirmed explicitly by substituting the solution to the right-hand sides of Eqs. (40) and (41). Thus, the marginal probability $\Pr\{S_{ij} = 1 \mid u\}$ at every edge $\{i, j\}$ is equal to $1/2$ for $u = 1$.

Expanding $\lambda_{i\to\{i,j\}}(s)$ in powers of $\ln(u)$ in Eqs. (40) and (41) and retaining only the first order terms, we obtain

$$\begin{cases} \lambda_{i\to\{i,j\}}(1) = \dfrac{1}{2} + \dfrac{1}{8}\ln(u) + \mathcal{O}((\ln(u))^2) & (i \in V\backslash\partial V) \\ \lambda_{i\to\{i,j\}}(1) = \dfrac{1}{2} + \dfrac{3}{8}\ln(u) + \mathcal{O}((\ln(u))^2) & (i \in \partial V,\ j \in \partial V,\ \partial i\backslash\{j\} \subset V\backslash\partial V) \\ \lambda_{i\to\{i,j\}}(1) = \dfrac{1}{2} + \dfrac{5}{8}\ln(u) + \mathcal{O}((\ln(u))^2) & (i \in \partial V,\ j \in \partial V,\ \partial i\backslash\{j\} \subset \partial V) \\ \lambda_{i\to\{i,j\}}(1) = \dfrac{1}{2} + \dfrac{7}{8}\ln(u) + \mathcal{O}((\ln(u))^2) & (i \in \partial V,\ j \in V\backslash\partial V,\ \partial i\backslash\{j\} \subset \partial V) \end{cases} \tag{49}$$

for $u \to 1$ and infinitesimally small $\ln(u)$. In the above derivations, we introduce $\delta\lambda_{i\to\{i,j\}}(s) \equiv \lambda_{i\to\{i,j\}}(s) - \frac{1}{2}$ and substitute $\lambda_{i\to\{i,j\}}(s) \equiv \frac{1}{2} + \delta\lambda_{i\to\{i,j\}}(s)$ into Eqs. (40) and (41). In the above calculations, we consider infinitesimal deviations of order $\ln(u)$ of the messages $\delta\lambda_{i\to\{i,j\}}(s)$.

By substituting the above asymptotic forms of Eq. (49) to Eq. (39), we obtain the following asymptotic behavior for the marginal probability $\Pr\{S_{ij} = 1 \mid u\}$:

$$\begin{aligned} \Pr\{S_{ij} = 1 \mid u\} &= \frac{1}{2} + \delta\lambda_{i\to\{i,j\}}(1) + \delta\lambda_{j\to\{i,j\}}(1) + \cdots \\ &= \begin{cases} \dfrac{1}{2} + \dfrac{1}{4}\ln(u) + \mathcal{O}((\ln(u))^2) & (i \in V\backslash\partial V, j \in V\backslash\partial V) \\ \dfrac{1}{2} + \ln(u) + \mathcal{O}((\ln(u))^2) & (i \in \partial V, j \in V, \partial i\backslash\{j\} \subset \partial V) \quad (u \to 1) \\ \dfrac{1}{2} + \dfrac{1}{2}\ln(u) + \mathcal{O}((\ln(u))^2) & (i \in \partial V, \partial i \subset V\backslash\partial V) \end{cases} \end{aligned} \tag{50}$$

In the case of infinitesimal positive $\ln(u)$, we see that the marginal probability $\Pr\{S_{ij} = 1 \mid u\}$ of each edge $\{i, j\}$ with $i, j \in V\backslash\partial V$ is larger than the one of each edge $\{i, j\}$ with $i \in \partial V$ or $j \in \partial V$. Thus the average of marginals $\frac{1}{|E|}\sum_{\{i,j\}\in E}\Pr\{S_{ij} = 1 \mid u\}$ becomes larger with the ratio $|\partial V|/|E|$ increasing. In the case of infinitesimal negative $\ln(u)$

such that $u \to 1-0$, we see that the values of the marginal probability at each edge $\{i,j\}$ consisting of inner vertices $i,j(\in V\backslash\partial V)$ are smaller than those of edges $\{i,j\}$ including boundary vertex, i.e. $i \in \partial V$ or $j \in \partial V$. In this case the average of the marginals $\frac{1}{|E|}\sum_{\{i,j\}\in E}\Pr\{S_{ij}=1 \mid u\}$ becomes smaller with increasing $|\partial V|/|E|$.

The above perturbative analysis thus explains the numerically observed behavior around $u=1$. Indeed, in Figs. 15 and 16, it was shown that $\frac{1}{|E|}\sum_{\{i,j\}\in E}\Pr\{S_{ij}=1 \mid u\}$ is equal to $1/2$ both in the exact diagrammatical method and the LBP. Moreover, in both the exact calculation and the LBP, $\frac{1}{|E|}\sum_{\{i,j\}\in E}\Pr\{S_{ij}=1 \mid u\}$ increases with infinitesimal positive $\ln(u)$ and decreases with infinitesimal negative $\ln(u)$ when the ratio $|\partial V|/|E|$ increases.

8. Concluding Remarks

In the present paper, we have considered undirected planar graphs such that the degree of every vertex is restricted to two or three and have introduced probabilistic models for single connected cycles. By using the diagrammatical method, we have obtained the exact expression for $\frac{1}{|E|}\sum_{\{i,j\}\in E}\Pr\{S_{ij}=1 \mid u\}$. We have also derived the approximate marginal probability $\Pr\{S_{ij}=1 \mid u\}$ by using LBP. The comparison between the exact result and the approximate result show that LBP gives us good accuracy except for a region near the transition point of the present probabilistic model. In particular, at $u=1$ all marginals are equal to $1/2$ for all finite as well as the infinite honeycomb lattice, and we find the LBP results to be exact. For larger u-values LBP does no longer lead to exact, but rather good approximate results for all finite and the infinite lattice. However, below the transition point at $u=1$, LBP and the exact diagrammatical method lead to quite different results. This was numerically observed on lattices of finite size. Instead, for the infinite lattice we analytically found different values for the transition point.

Our formulation of the diagrammatical method can be used to calculate the marginal probabilities $\Pr\{S_{ij}=1 \mid u\}$ of the present model also on planar random graphs for which the degree of every vertex is either two or three. This implies that it is interesting to find the class of solvable probabilistic models as the diagrammatical method can then be used to reveal properties regarding their cycles. This could be of interest when modeling the network structures found in nature by random ones [20, 27].

The above analysis can be extended to a calculation of the single marginal probabilities $\Pr\{S_{ij}=1 \mid u\}$ for each edge $\{i,j\}\in E$ by considering the following partition function:

$$Z(\{u_{ij} \mid \{i,j\}\in E\}) \equiv \sum_{\boldsymbol{s}}\left(\prod_{\{i,j\}\in E} u_{ij}^{s_{ij}}\right)\left(\prod_{i\in V}\left(\delta\left(\sum_{k\in\partial i} s_{ik},0\right)+\delta\left(\sum_{k\in\partial i} s_{ik},2\right)\right)\right). \tag{51}$$

Here each u_{ij} depends on the edge $\{i,j\}$. By differentiating $Z(\{u_{ij} \mid \{i,j\}\in E\})$ with respect to u_{ij}, we obtain

$$\begin{aligned}\Pr\{S_{ij}=1 \mid \{u_{ij}\}\} &= \left(\frac{1}{u_{ij}}\right)\frac{\partial}{\partial u_{ij}}\ln Z(\{u_{ij} \mid \{i,j\}\in E\}).\\ &= \frac{1}{2u_{ij}}\mathrm{Tr}\left((\boldsymbol{I}-\boldsymbol{\Lambda})^{-1}\frac{\partial}{\partial u_{ij}}(\boldsymbol{I}-\boldsymbol{\Lambda})\right).\end{aligned} \tag{52}$$

The partition function $Z(\{u_{ij} \mid \{i,j\}\in E\})$ in Eq. (51) can be expressed as Eq. (15) in terms of the matrix $\boldsymbol{I}-\boldsymbol{\Lambda}$ defined by replacing u by u_{ij} in Eq. (12). It is interesting to calculate the marginal probabilities $\Pr\{S_{ij}=1 \mid \{u_{ij}\}\}$ for various random planar graphs for which the degree of every vertex is either two or three. It remains also one of future problems.

In the present paper, we showed the result for the marginal probability obtained by means of the LBP for the honeycomb lattice with an infinite number of vertices. The result is very close to the exact results except for the region near the transition point. In the future it would be interesting to discuss the dependency of the accuracy of LBP due to finite size effects more qualitatively.

Also, it would be interesting to analyze the behaviour of the probabilistic models on planar graphs for which the degree of the vertices can be more than three. In such cases, there still exist some solvable probabilistic models. One of them is a vertex model with free fermion conditions [6, 7, 10, 11, 13–16]. However, the present probabilistic model of Eqs. (1) and (2) does not satisfy free fermion conditions on planar graphs if the degree for each vertex is four. Thus, the present probabilistic model would have to be modified so as to satisfy a free fermion condition at every vertex.

In the present paper, we calculate a marginal probability $\Pr\{S_{ij}=1 \mid u\}$ for every edge $\{i,j\}\in E$. In the problem of finding long cycles in random graphs, we may have to calculate a probability that every vertex includes the same cycle. In the large u limit, this corresponds to the probability that a Hamiltonian cycle exists in a given graph. Hence, it is interesting to investigate this probability for the present probabilistic model.

Acknowledgments

This work was partly supported by the Grants-In-Aid (No. 18079002) and the Global COE (Center of Excellence) Program "Center of Education and Research for Information Electronics Systems" for Scientific Research from the Ministry of Education, Culture, Sports, Science and Technology of Japan.

REFERENCES

[1] Monasson, R., Zecchina, R., Kirkpatrick, S., Selman, B., and Troyansky, L., "Determining computational complexity from characteristic 'phase transitions'," *Nature*, **400**: 133 (1999).
[2] Martin, O. C., Monasson, R., and Zecchina, R., "Statistical mechanics methods and phase transitions in optimization problems," *Theoretical Computer Science*, **265**: 3 (2001).
[3] Mézard, M., Parisi, G., and Zecchina, R., "Analytic and algorithmic solution of random satisfiability problems," *Science*, **297**: 812 (2002).
[4] Marinari, E., Semerjian, G., and Van Kerrebroeck V., "Finding long cycles in graphs," *Physical Review E*, **75**: 066708 (2007).
[5] Marinari, E. and Van Kerrebroeck, V., "Cycles in sparse random graphs," *Journal of Physics: Conference Series*, **95**: 012014 (2007).
[6] Fan, C. and Wu, F. Y., "Ising model with second-neighbor interaction. I. Some exact results and an approximate solution," *Physical Review*, **179**: 560 (1969).
[7] Fan, C. and Wu, F. Y., "General lattice model of phase transitions," *Physical Review B*, **2**: 723 (1970).
[8] Wu, F. Y., "Eight-vertex model on the honeycomb lattice," *Journal of Mathematical Physics*, **15**: 687 (1974).
[9] Wu, F. Y., "Eight-vertex model and Ising model in a non-zero magnetic field: honeycomb lattice," *Journal of Physics A: Mathematical and General*, **23**: 375 (1990).
[10] Wiegel, F. W., "Combinatorial solution of the free fermion model," *Physics Letters A*, **41**: 225 (1972).
[11] Wiegel, F. W., "Combinatorial solution of the free fermion model," *Canadian Journal of Physics*, **53**: 1148 (1975).
[12] Morita, T., "Justification of Vdovichenko's method for the Ising model on a two-dimensional lattice," *Journal of Physics A: Mathematical and General*, **19**: 1197 (1986).
[13] Tanaka, K. and Morita, T., "Free energy for layered free fermion models," *Journal of the Physical Society of Japan*, **61**: 92 (1982).
[14] Morita, T. and Tanaka, K., "Diagrammatical techniques for two-dimensional Ising models. III. Ising Model to Vertex Model," *Journal of the Physical Society of Japan*, **62**: 873 (1993).
[15] Samuel, S., "The use of anticommuting variable integrals in statistical mechanics. I. The computation of partition functions," *Journal of Mathematical Physics*, **21**: 2806 (1980).
[16] Samuel, S., "The use of anticommuting variable integrals in statistical mechanics. II. The computation of correlation functions," *Journal of Mathematical Physics*, **21**: 2815 (1980).
[17] Chertkov, M. and Chernyak, V. Y., "Loop calculus in statistical physics and information science," *Physical Review E*, **73**: 065102(R) (2006).
[18] Brézin, E., Itzykson, C., Parisi, G., and Zuber, J. B., "Planar diagrams," *Communications in Mathematical Physics*, **59**: 35 (1978).
[19] Mehta, M. L., "A method of integration over matrix variables," *Communications in Mathematical Physics*, **79**: 327 (1981).
[20] Johnston, D. A., "Symmetric vertex models on planar random graphs," *Physics Letters B*, **463**: 9 (1999).
[21] Globerson, A. and Jaakkola, T., *Advances in Neural Information Processing Systems*, **19**: 473 (MIT Press, 2007).
[22] Chertkov, M., Chernyak, V. Y., and Teodorescu, R., "Belief propagation and loop series on planar graphs," *Journal of Statistical Mechanics: Theory and Experiment*, P05003 (2008).
[23] Morita, T., "Reentrant transition of the Ising model on the centred square lattice," *Journal of Physics A: Mathematical and General*, **19**: 1701 (1986).
[24] Opper, M. and Saad, D. (eds), *Advanced Mean Field Methods —Theory and Practice—* (MIT Press, 2001).
[25] Yedidia, J. S., Freeman, W. T., and Weiss, Y., "Constructing free-energy approximations and generalized belief propagation algorithms," *IEEE Transactions on Information Theory*, **51**: 2282 (2005).
[26] Pelizzola, A., "Cluster variation method in statistical physics and probabilistic graphical models (Topical Review)," *Journal of Physics A: Mathematical and General*, **38**: R309 (2005).
[27] Bianconi, G., Coolen, A. C. C., and Perez Vicente, C. J., "Entropies of complex networks with hierarchically constrained topologies," *Physical Review E*, **78**: 016114 (2008).